THE JOURNAL OF BIOLOGICAL CHEMISTRY
Vol. 278, No. 48, Issue of November 28, pp. 47898–47904, 2003
Printed in U.S.A.

Identification of a Surface for Binding to the GDNF-GFRα1 Complex in the First Cadherin-like Domain of RET*[S]

Received for publication, September 3, 2003, and in revised form, September 24, 2003
Published, JBC Papers in Press, September 26, 2003, DOI 10.1074/jbc.M309772200

Svend Kjær and Carlos F. Ibáñez‡

From the Division of Molecular Neurobiology, Department of Neuroscience, Karolinska Institute, 171 77 Stockholm, Sweden

The RET receptor tyrosine kinase is activated by binding to a ligand complex formed by a member of the glial cell line-derived neurotrophic factor (GDNF) family of neurotrophic factors bound to its cognate GDNF-family receptor-α (GFRα) glycosylphosphatidylinositol-linked co-receptor. Molecular modeling studies of the extracellular domain of RET (RET^{ECD}) have revealed the existence of four cadherin-like domains (CLD1–4) followed by a cysteine-rich domain. Cross-linking experiments have indicated that the RET^{ECD} makes direct contacts with both the GDNF ligand and GFRα1 molecule in the complex, although it has low or no detectable affinity for either component alone. We have exploited sequence and functional divergences between the ectodomains of mammalian and amphibian RET molecules to map binding determinants in the human RET^{ECD} responsible for its interaction with the GDNF-GFRα1 complex by homologue-scanning mutagenesis. We found that *Xenopus* RET^{ECD} was unable to bind to GDNF-GFRα-1 or neurturin (NTN)-GFRα-2 complexes of mammalian origin. However, a chimeric molecule containing CLD1, -2, and -3 from human RET^{ECD}, but neither domain alone, had similar binding activity as compared with wild type human RET^{ECD}, suggesting the existence of an extended ligand binding surface within the three N-terminal cadherin-like domains of human RET^{ECD}. Subsequent loss-of-function experiments at higher resolution identified three small subsets of residues, mapping on the same face of the molecular model of RET CLD1, that were required for the interaction of human RET^{ECD} with the GDNF-GFRα1 complex. Additional experiments demonstrated that *N*-linked glycosylation of human RET^{ECD} was not required for ligand binding. Based on these observations, we propose a model for the assembly and architecture of the GDNF-GFRα1-RET complex.

Glial cell line-derived neurotrophic factor (GDNF)[1] was initially identified as a potent survival factor of ventral midbrain dopaminergic neurons (1) and has since its discovery been intensely studied due to its potential utility as a therapeutic agent for the treatment of neurodegenerative diseases, such as Parkinson's disease (2). GDNF is a disulfide-linked homodimer consisting of two polypeptide chains of about 110 residues each. The overall disulfide arrangement of GDNF conforms to the structural cystine knot motif (3). Sequence and structural similarities have indicated that GDNF is a distant member of the transforming growth factor-β superfamily of ligands. However, unlike typical members of this family that signal through receptor serine-threonine kinases, GDNF signals through a receptor complex formed by the receptor tyrosine kinase RET and a glycosylphosphatidylinositol-anchored, ligand binding moiety, the GDNF family receptor α1 (GFRα1). Four structurally related but distinct ligands, namely GDNF, neurturin (NTN), persephin, and artemin, utilize RET as signaling receptor with the aid of four different GFRα receptors (GFRα1–4), which confer ligand specificity (4, 5). In addition, an alternative receptor complex for GDNF family ligands, involving the neural cell adhesion molecule in collaboration with GFRα proteins, has recently been identified (6).

Both gain- and loss-of-function mutations in the *RET* gene have been identified in human diseases. Mutations inducing constitutive dimerization or activation of the RET tyrosine kinase lead to familial and sporadic cancers in neuroendocrine organs, including multiple endocrine neuroplasias type 2A and 2B and familial medullary thyroid carcinoma (7, 8). Loss-of-function mutations in RET cause a dominant genetic disorder of neural crest development known as Hirschsprung disease, which results in a lack of neurons in distal segments of the enteric nervous systems and colon aganglionosis (9). Although RET has no detectable affinity for any of the GDNF family ligands in the absence of GFRα receptors, chemical cross-linking and co-immunoprecipitation experiments have indicated that RET can still make direct contacts with both the GDNF and GFRα1 molecules in the complex (10–12). A structural and functional understanding of the protein-protein interactions at play in the GDNF-GFRα1-RET ternary complex is still lacking and will be required for the rational design of small molecules capable of mimicking the effects of GDNF.

The binding determinants that mediate the interaction between GDNF family ligands and GFRα molecules have been investigated using different approaches, including alanine and homologue-scanning mutagenesis (12–14). Key residues involved in the interaction with GFRα receptors were found in the two β−hairpin "fingers" of the GDNF molecule (13, 14). Intriguingly, residues at analogous positions have been shown to participate in the interaction of classical transforming

* This work was supported by grants from the Swedish Foundation for Strategic Research, the Swedish Medical Research Council (K99-33X-10908-06C), the Vth Framework Program of the European Union (QLRT-1999-00099), Centrala Försökdjursnämnden, the Swedish Fund for Research without Laboratory Animals, and the Karolinska Institute. The costs of publication of this article were defrayed in part by the payment of page charges. This article must therefore be hereby marked "*advertisement*" in accordance with 18 U.S.C. Section 1734 solely to indicate this fact.

[S] The on-line version of this article (available at http://www.jbc.org) contains a supplementary figure showing surface accessibility plots of CLDs 1, 2, and 3 of the human RET^{ECD}.

‡ To whom correspondence should be addressed. carlos.ibanez@neuro.ki.se.

[1] The abbreviations used are: GDNF, glial cell line-derived neurotrophic factor; GFRαa, GDNF-family receptor-α; NTN, neurturin; CLD, cadherin-like domains; HA, hemagglutinin; PBS, phosphate-buffered saline; TBS, Tris-buffered saline; PNGase F, peptide:*N*-glycosidase F; Endo H, endoglycosidase H.

growth factor-β proteins with their cognate type II receptors (15). The major determinant of ligand binding in GFRα molecules has been localized to the most conserved region of the molecule, a central domain predicted to contain four conserved α-helices and two short β-strands (12). Distinct hydrophobic and positively charged residues in this central region were required for the binding of GFRα1 to GDNF (12). Because the RET^{ECD} is unable to bind members of the GDNF family directly, and only weakly to GFRα molecules (16), this receptor is likely to interact with a composite surface formed by residues from both GDNF and GFRα molecules. However, the regions and residues in RET^{ECD} that participate in these interactions have remained unknown.

The overall molecular architecture of the RET^{ECD} was recently elucidated using a bioinformatics approach (17). In that study, it was found that the RET^{ECD} comprises four N-terminal domains with similarity to classical cadherin molecules, so-called cadherin-like domains or CLDs, followed by a C-terminal cysteine-rich domain. Multiple alignments indicate that the RET^{ECD} from a number of different species, including human, mouse, chick, frog, fish, and fly, appear to conform to this organization (17). The highest degree of sequence similarity between the RET^{ECD} and cadherins is found in and around a highly conserved calcium binding site present between CLD2 and CLD3 but, unlike classical cadherins, absent between all other RET^{ECD} subdomains (17).

In the present study, we have investigated the location and biochemical characteristics of ligand binding determinants in the human RET^{ECD}. For this purpose, we have employed homologue-scanning mutagenesis, taking advantage of the inability of the *Xenopus* RET^{ECD} to interact with complexes between GDNF family ligands and GFRα molecules of mammalian origin, despite its overall structural similarity to the human RET^{ECD}.

MATERIALS AND METHODS

DNA Constructs—All expression constructs were generated in the pSecTag2AHA system (18). The cDNA encoding the mature part of the RET ectodomain was amplified by PCR and cloned into the *SfiI* and *NotI* sites of the pSecTag2AHA vector. The chimeric constructs were generated by splicing by overlap extension (19). The integrity of the cloning junctions of all constructs were confirmed by automated DNA sequencing. The regions targeted for mutation by en-bloc mutagenesis were identified using the GETAREA 1.1 software (20) (www.scsb.utmb.edu/getarea/area_man.html) with the coordinates from the modeled CLD (1–3) as input (17).

Transfection and Selection of Stable CHO Cell Lines—Chinese hamster ovary (CHO) cells were maintained in a humid atmosphere of 5% CO_2 in Dulbecco's modified Eagle's medium (Invitrogen) supplemented with 2 mM L-glutamine and 60 μg/ml gentamycin and 10% fetal bovine serum. Freshly split CHO cells were transfected using FuGENE 6 with the different chimeric constructs. Forty-eight h after transfection, 800 μg/ml of hygromycin B (Invitrogen) was applied in complete Dulbecco's modified Eagle's medium. Colonies were picked within 1–2 weeks of selection and expanded in 96-well plates. The expression of RET protein was determined by Western blot using the anti-HA antibody B16.12 (Covance, Biosite) as primary antibody. Single clones were expanded for expression experiments.

Expression of Soluble Chimeric RET^{ECD} Proteins—Stably transfected CHO cells were expanded into 10-cm plates and allowed to reach 80% confluence. Subsequently, the serum-containing medium was removed, and the cells were rinsed twice with PBS. Serum-free medium consisting of Dulbecco's modified Eagle's medium supplemented with 2 mM L-glutamine and 1 mM Hepes and 60 μg/ml gentamycin was added to the cells. To enhance the yield, prevent CHO cell proliferation, and alleviate potential misfolding routes during protein maturation, the CHO cells were expanded at 37 °C but shifted to 30 °C for the period of protein expression in serum-free medium as described previously (18). The incubation and protein production were continued for 3–4 days at +30 °C. The serum-free medium was concentrated using Centriprep-10 (Amicon). The concentration of the protein was determined either by Western blotting with anti-HA antibodies or by sandwich enzyme-linked immunosorbent assay using anti-HA antibodies as capture tools and a polyclonal rabbit anti-RET^{ECD} antibody (18) as detection reagent.

Deglycosylation Assays—To verify the structural integrity (and consequent ability of the molecules to pass the "quality control checkpoint" of the endoplasmic reticulum) of the RET domain chimeras and fine-tuned mutants, the chimeric RET^{ECD} mutants were subjected to deglycosylation assays using endoglycosidase H (Endo H) and peptide:*N*-glycosidase F (PNGase F) deglycosidases. Typically, 50 μl of conditioned medium was either treated with deglycosidase or left untreated. The deglycosylation was carried out according to instructions of the manufacturer (New England Biolabs).

Binding Assays—The binding experiments were performed essentially as described (18). Briefly, 50 ng of human GDNF (PeproTech) was mixed with 250 ng of a fusion protein formed by rat GFRα1 and the Fc domain of human IgG (GFRα1-Fc, R&D Systems) in PBS. In some experiments, the related ligand NTN (human) and the Fc fusion of its cognate GFRα2 receptor (from rat) were also used. After 5 min of incubation at room temperature, the protein solution was added to the wells of an enzyme-linked immunosorbent assay plate (MaxiSorp, Nunc). The following day, the wells were rinsed by PBS and blocked with 2% skimmed milk powder in TBS (2% MTBS) for 1 h at room temperature. Equal amounts of RET^{ECD} mutants were added to the GDNF-GFRα-1-Fc coated wells and to wells only coated with 2% MTBS. The binding was allowed to proceed for 1 h at room temperature. The washing was performed with TBS with 0.1% Tween 20 three times and TBS three times. Following washing, bound RET^{ECD} molecules were detected by a monoclonal anti-HA antibody at a 1:2000 dilution in 2% MTBS. Finally, the monoclonal anti-HA antibody was detected with an anti-mouse horseradish peroxidase-conjugated antibody (DAKO) at a 1:2000 dilution in MTBS. The reaction was developed by addition of 3,3′,5,5′-tetramethyl benzidine (TMB) substrate according to the instructions of the manufacturer (Pierce).

Native Deglycosylation of Human RET^{ECD} and Binding Analysis—To examine the influence of the *N*-linked carbohydrates attached to the ectodomain of RET, the carbohydrates were enzymatically removed under native conditions. Briefly, 1 μg of semipurified HA-tagged RET^{ECD} was deglycosylated by incubation with 20 units of PNGase F overnight at 4 °C. Half of the reaction was applied for binding experiments as described above. The remaining portion was taken for Western blot analysis to verify the removal of *N*-linked carbohydrates.

RESULTS

Preferential Interaction of the Mammalian GDNF-GFRα-1 Ligand Complex with Human, but Not Xenopus, RET^{ECD}—To evaluate the functional capabilities of wild type and mutant RET^{ECD} molecules, we have developed a solid-phase binding assay using immobilized human GDNF, rat GFRα1, or the GDNF-GFRα1 complex as target ligands (18). Recombinant RET^{ECD} molecules were produced as epitope-tagged, soluble proteins in serum-free supernatants of stable transfected CHO cell lines as described previously (18). As shown in Fig. 1*A*, human RET^{ECD} was able to detect the GDNF-GFRα1 complex with an EC_{50} of ~0.2 nM, a value comparable with the binding affinity reported previously using cell-based cross-linking binding assays (10). The human RET^{ECD} did not interact with either GDNF or GFRα1 alone (Fig. 1*A*), in agreement with previous observations. Similar to cell-based binding assays (17, 21, 22), the interaction between the human RET^{ECD} and the GDNF-GFRα1 complex in our solid-phase binding assay was dependent on Ca^{2+}, as it was totally abolished in the presence of 1 mM of the Ca^{2+}-specific chelator EGTA (Fig. 1*B*). Based on its structural role in the cadherin molecule, the binding of Ca^{2+} ions to the CLD2/CLD3 interface of the RET^{ECD} is thought to rigidify the relative orientations of these two cadherin-like domains in RET^{ECD} (23, 24). The requirement of Ca^{2+} for the ability of the RET^{ECD} to interact with the GDNF-GFRα1 complex suggests that residues located on both sides of the Ca^{2+} binding site between CLD2 and CLD3 may contribute to ligand binding. Despite its overall structural similarity to human RET^{ECD} (17), the *Xenopus* RET^{ECD} has only 45% amino acid identity to its human counterpart, indicating a significant level of sequence divergence between the two species. In contrast, the intracellular domains of human and *Xenopus* RET display

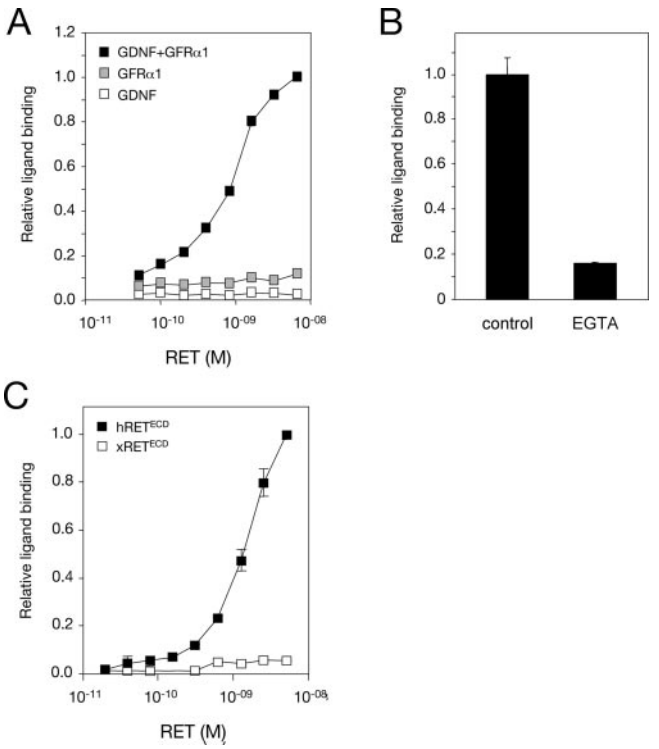

FIG. 1. **Preferential interaction of the mammalian GDNF-GFRα1 ligand complex with human, but not *Xenopus*, RET^{ECD}.** *A*, solid-phase binding assay of human RET^{ECD} with immobilized human GDNF (*open squares*), rat GFRα1 (*gray squares*), or a GDNF-GFRα1 complex (*solid squares*). Shown are the means of triplicate observations. *B*, solid-phase binding assay of human RET^{ECD} with immobilized GDNF-GFRα1 complex in control conditions or in the presence of the Ca^{2+} chelator EGTA. Shown are the means of triplicate observations. *C*, solid-phase binding assay of human (*solid squares*) or *Xenopus* (*gray squares*) RET^{ECD} with immobilized GDNF-GFRα1. Shown are means ± S.D. of triplicate observations.

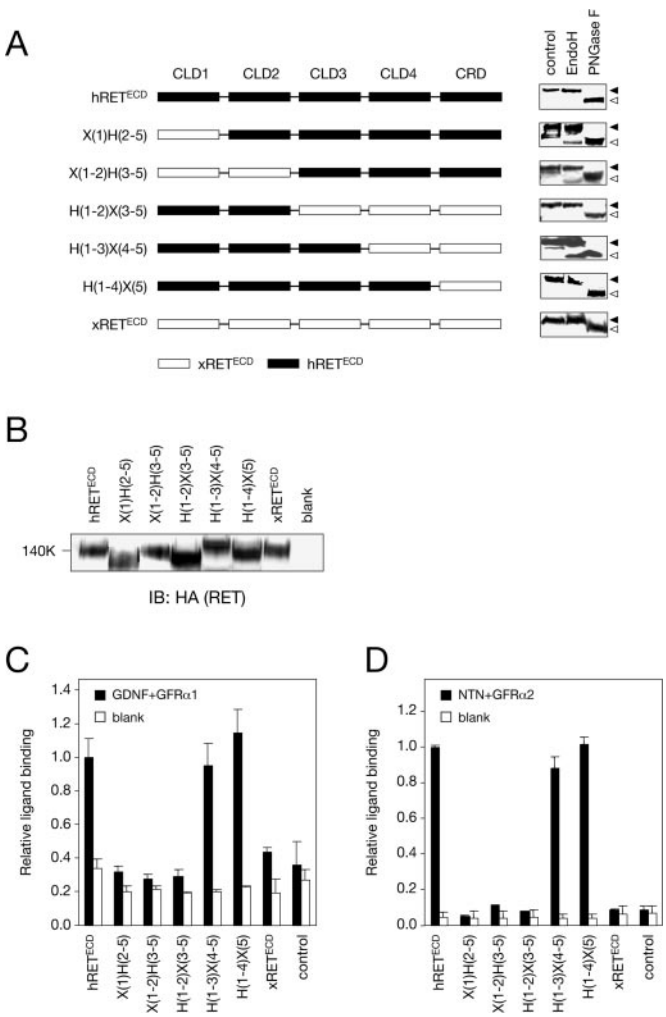

FIG. 2. **CLD1, -2, and -3 of the human RET^{ECD} are required for binding to the mammalian GDNF-GFRα1 ligand complex.** In *A*, chimeric RET^{ECD} constructs produced in supernatants of stably transfected CHO cells grown at 30 °C were subjected to deglycosylation as indicated. RET^{ECD} proteins were detected with an anti-HA antibody. Deglycosylation-resistant (*solid arrowheads*) and -sensitive (*empty arrowheads*) protein species are indicated. All constructs were sensitive to PNGase F digestion, as expected, but were largely resistant to Endo H. The diagram summarizes the chimeric molecules generated and their corresponding nomenclature. *h*, human; *x*, *Xenopus*. *B*, anti-HA tag blot of CHO cell supernatants showing that chimeric molecules were produced at comparable levels. *IB*, immunoblot. *C*, solid-phase binding assay of chimeric RET^{ECD} molecules. Wells were coated with GDNF-GFRα1-Fc complex (*solid bars*) or PBS (*white bars*) and subsequently blocked with low-fat milk. Results were normalized to the binding of wild type human RET^{ECD}. *Control* denotes supernatant from mock-transfected CHO cells. Shown are means ± S.D. of triplicate observations. *D*, solid-phase binding assay of chimeric RET^{ECD} molecules. Wells were coated with NTN-GFRα2-Fc complex (*solid bars*) or PBS (*white bars*) and subsequently blocked with low-fat milk. Shown are means ± S.D. of triplicate observations.

greater than 85% sequence identity. When compared with human RET^{ECD}, *Xenopus* RET^{ECD} showed negligible binding to the mammalian GDNF-GFRα1 complex in the concentration range tested (Fig. 1*C*), indicating that divergent regions between human and *Xenopus* RET^{ECD} may represent specific ligand binding determinants.

A Strategy for Homologue-scanning Mutagenesis of the Human RET^{ECD}—The inability of *Xenopus* RET^{ECD} to interact with the mammalian GDNF-GFRα1 complex despite its overall structural similarity to the human RET^{ECD} allowed us to use a homologue-scanning mutagenesis approach to study structure-function relationships in the RET^{ECD}. Based on the subdomain boundaries defined in a previous bioinformatics study on the RET^{ECD} (17), a series of chimeric molecules was constructed by swapping different subdomains between human and *Xenopus* RET^{ECD} (Fig. 2*A*). Stable CHO cell lines secreting different epitope-tagged chimeric *Xenopus*/human RET^{ECD} molecules were generated as described previously (18).

In a previous study, we found that certain subdomains of the RET^{ECD}, mainly CLD1, -2, and -3, have an intrinsic susceptibility to misfolding that makes them particularly vulnerable to inactivating mutations such as those found in patients with Hirschsprung disease (18). Misfolded RET^{ECD} molecules are retained intracellularly in the endoplasmic reticulum and eventually ubiquitinated and degraded, although a fraction may also get access to the extracellular space by direct leakage from the endoplasmic reticulum, particularly after overexpression (18). Folded and misfolded RET^{ECD} molecules can be distinguished by the sensitivity of the latter to Endo H (18). Upon exit from the endoplasmic reticulum, correctly folded glycoproteins lose sensitivity to Endo H as carbohydrates of higher complexity are added in the Golgi complex. The structural integrity of chimeric RET^{ECD} molecules was examined by subjecting the secreted proteins to Endo H treatment as described previously (18). As a control, RET^{ECD} proteins were treated with PNGase F, which removes sugars from both folded and misfolded proteins. As shown in Fig. 2*A*, all chimeric RET^{ECD} proteins were resistant to Endo H treatment (*solid arrowheads*) but were still sensitive to PNGase F as expected (*open arrowheads*). These results indicated that this set of *Xenopus*/human chimeric RET^{ECD} molecules was folded correctly.

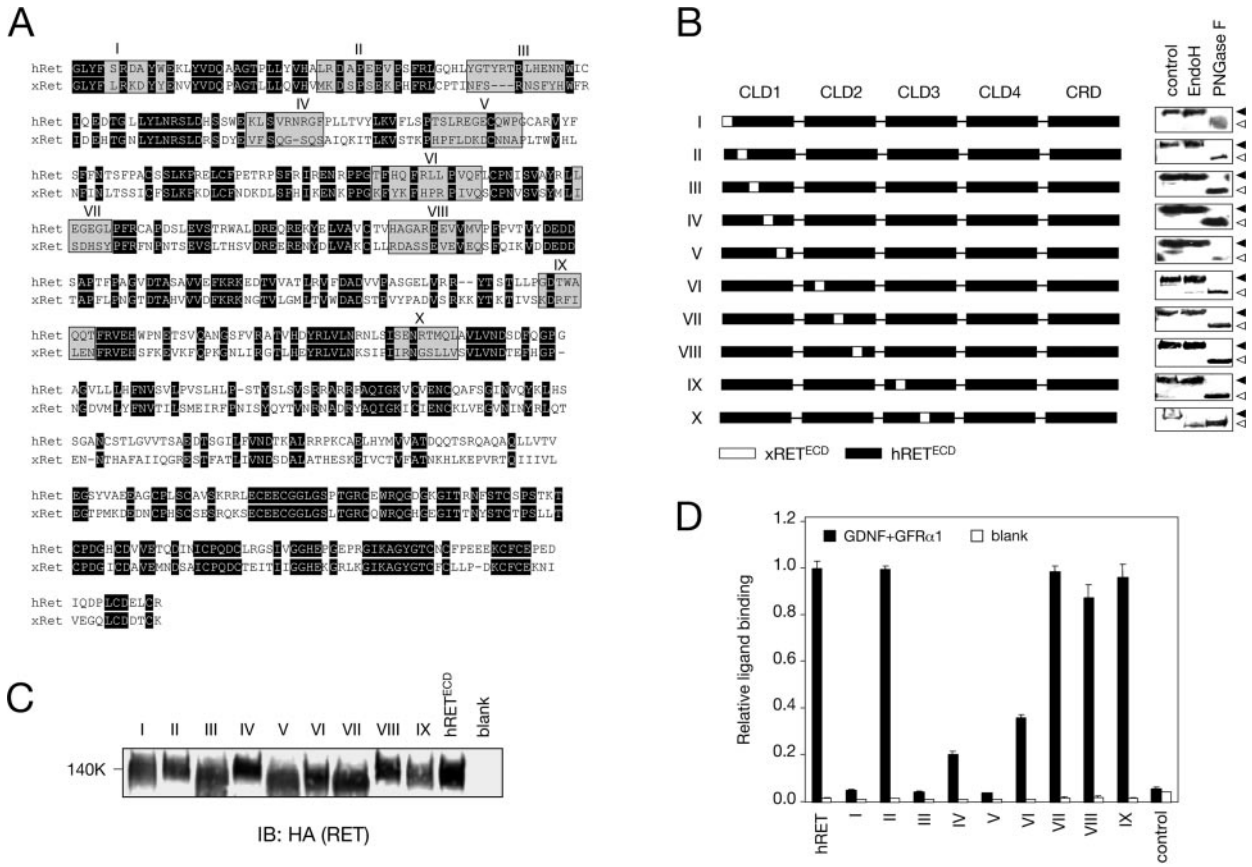

FIG. 3. **Distinct clusters of exposed residues in CLD1 are required for binding of human RET^{ECD} to the GDNF-GFRα1 complex.** *A*, alignment of the human and *Xenopus* RET^{ECD} with conserved residues *boxed* in *black*, and surface-exposed, variable regions used to produce chimeric molecules *boxed* in *gray*. *hRet*, human RET; *xRet*, *Xenopus* RET. In *B*, chimeric RET^{ECD} constructs produced in supernatants of stably transfected CHO cells grown at 30 °C were subjected to deglycosylation as indicated. RET^{ECD} proteins were detected with an anti-HA antibody. Deglycosylation-resistant (*solid arrowheads*) and -sensitive (*empty arrowheads*) species are indicated. All constructs were sensitive to PNGase F digestion, as expected. Constructs I–IX were largely resistant to Endo H, whereas construct X was sensitive, indicating a misfolded protein. The diagram summarizes the chimeric molecules generated and their corresponding nomenclature. *C*, anti-HA tag blot of CHO cell supernatants showing that wild type hRET^{ECD} and chimeric molecules I–IX were produced at comparable levels. *IB*, immunoblot. *D*, solid-phase binding assay of chimeric RET^{ECD} molecules. Wells were coated with GDNF-GFRα1-Fc complex (*solid bars*) or PBS (*white bars*) and subsequently blocked with low-fat milk. Results were normalized to the binding of wild type human RET^{ECD}. *Control* denotes supernatant from mock-transfected CHO cells. Shown are means ± S.D. of triplicate observations.

CLD1, -2, and -3 of the Human RET^{ECD} Are Required for Binding to the Mammalian GDNF-GFRα1 Ligand Complex—The ligand binding activity of chimeric RET^{ECD} proteins was evaluated using a solid-phase binding assay with the GDNF-GFRα1 complex immobilized to 96-well plates. Chimeric molecules were also tested against a complex formed by human NTN and rat GFRα2. Equivalent levels of wild type and chimeric proteins were present in these experiments as demonstrated by Western blotting using an antibody against the HA epitope tag present in all the constructs (Fig. 2*B*). *Xenopus* RET^{ECD} was not able to interact with the NTN-GFRα2 complex (data not shown). As shown in Fig. 2, *C* and *D*, binding activity to either ligand complex required all three N-terminal cadherin-like domains of RET^{ECD} (*i.e.* CLD1, -2, and -3) to be of human origin. In contrast, the species of origin of CLD4 and the cysteine-rich domain had no impact on the ligand binding activity of chimeric RET^{ECD} molecules (Fig. 2, *C* and *D*). Similar structure-activity profiles were observed toward both GDNF-GFRα1 and NTN-GFRα2 complexes, indicating that the RET^{ECD} interacts with different members of the GDNF and GFRα families in a similar fashion. The fact that residues on both sides of the Ca^{2+} coordination site were required for ligand binding is in agreement with the recognized importance of Ca^{2+} for stabilizing the RET^{ECD} in a conformation competent for ligand binding and receptor activation (Fig. 1*B*) (17, 22).

Distinct Clusters of Exposed Residues in CLD1 Are Required for Binding of Human RET^{ECD} to the GDNF-GFRα1 Complex—Having established the existence of ligand binding determinants within CLD1, -2, and -3 of the human RET^{ECD}, we set out to define more precisely the location and identity of functionally important residues in these three domains. The GETAREA 1.1 program (www.scsb.utmb.edu/getarea/area_man.html) was used to generate surface accessibility plots of CLD1, -2, and -3 of the human RET^{ECD} using the coordinates of their modeled structures (17) (see the supplemental figure). Segments displaying more than 50% surface accessibility were examined for their degree of sequence similarity to analogous segments in the *Xenopus* RET^{ECD}. Exposed segments of 6–12 residues in CLD1, -2, and -3 of the human RET^{ECD} displaying more than 50% divergence from the equivalent *Xenopus* sequences were targeted for a second round of homologue-scanning mutagenesis (Fig. 3*A*). A total of 10 chimeric constructs (designated with the Roman numerals I–X) were generated and produced in the supernatants of stable CHO cell transfectants as above (Fig. 3*B*). With the exception of chimeric protein X, all other chimeras were resistant to Endo H digestion and therefore considered correctly folded (Fig. 3*B*). Equivalent amounts of wild type human RET^{ECD} and chimeric proteins I–IX (Fig. 3*C*) were compared for their ability to bind the mammalian GDNF-GFRα1 complex in a solid-phase based binding assay as above.

As shown in Fig. 3*D*, chimeras I, III, IV, V, and VI all displayed a reduction in binding as compared with the wild type human RET^{ECD}.

Chimeric protein I carries 4 amino acid replacements as compared with wild type human RET^{ECD}, namely S32L, D34K, A35D, and W37Y, suggesting that one or more of those positions are crucial for the interaction of the RET^{ECD} with the GDNF-GFRα1 complex. Based on the modeled structure of CLD1 (17), residues in region III are predicted to form part of a loop between the C and D β-strands of this domain. This exposed segment is shorter and highly divergent in the *Xenopus* RET^{ECD}, indicating that residues in this loop region may also contribute to the binding of the human RET^{ECD} to the GDNF-GFRα1 complex.

In contrast to chimeras I, III, and V, chimeric protein IV retained ~20% binding to the GDNF-GFRα1 complex (Fig. 3*D*). Of the 8 amino acid exchanges in this region, three involve the replacement of positively charged residues by uncharged residues (Fig. 3*A*), indicating that one or more of those charges are important for formation of the GDNF-GFRα1-RET complex. The complete absence of detectable binding in chimeric protein V indicates that one or more of the residues exchanged in this region are important for ligand binding. Of the 9 amino acid differences between the human and *Xenopus* sequences in this region, R133L and W139N may be the most significant ones as they involve residues that are enriched in known protein-protein interfaces (25). Finally, a 60% reduction in ligand binding was observed in chimeric protein VI (Fig. 3*D*), which involves 9 amino acid replacements in CLD2 (Fig. 3*A*). Of note, this was the only set of mutations outside CLD1 that affected the interaction of the RET^{ECD} with the GDNF-GFRα1 complex. Interestingly, three of the exchanges in this region involve the replacement of two polar and one uncharged residue by positively charged residues (Fig. 3*A*). Taken together, they indicate that although CLD1, -2, and -3 of human RET^{ECD} are all required for ligand binding, the most important determinants appear to be concentrated in CLD1, the most N-terminal subdomain of the human RET^{ECD}.

N-linked Carbohydrates in Human RET^{ECD} Are Dispensable for Ligand Binding—Protein glycosylation can have a modulatory effect on protein-protein interactions, and introduction of *N*-linked glycosylation sites has been used as a mutagenesis strategy (26). The human RET^{ECD} is abundantly *N*-glycosylated, but the role of this post-translational modification in ligand binding is unknown. Interestingly, predicted *N*-glycosylation sites in the human RET^{ECD} are not evenly distributed, but the majority (9 of 12) of them appear downstream of the Ca^{2+} coordination site, in accord with the location of ligand binding determinants in the CLD1. We treated the human RET^{ECD} with PNGase F under native conditions and examined its ability to bind to the GDNF-GFRα1 complex. Treatment with PNGase F resulted in complete deglycosylation of the native protein, comparable with that obtained after prior denaturation (Fig. 4*A*). As shown in Fig. 4*B*, RET^{ECD} incubated in deglycosylation buffer with or without PNGase F without prior denaturation showed no loss of binding as compared with a non-treated control. Denaturation prior to enzymatic deglycosylation resulted in complete loss of binding, as expected (Fig. 4*B*). Thus, *N*-linked carbohydrates are unlikely to play a role in the assembly of the RET-GDNF-GFRα1 complex and may instead be of importance for the folding and maturation of the RET^{ECD} in the secretory pathway, as suggested previously (18).

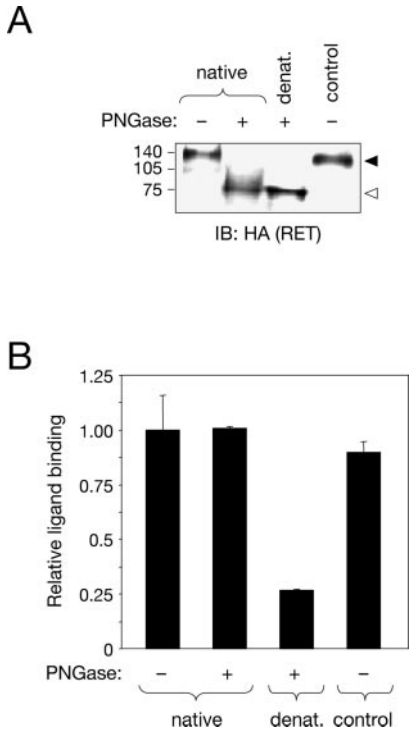

FIG. 4. ***N*-linked carbohydrates in human RET^{ECD} are dispensable for ligand binding.** In *A*, equal amounts of human RET^{ECD} were subjected to an incubation in the presence or absence of PNGase F under native or denaturing conditions as indicated. Untreated RET^{ECD} was used as control. *IB*, immunoblot. *B*, solid-phase binding assay of native and denatured human RET^{ECD} after treatment with PNGase as above. Wells were coated with GDNF-GFRα1-Fc complex. Shown are means ± S.D. of triplicate observations.

DISCUSSION

The receptor tyrosine kinase RET has remained in the limelight ever since its discovery as a transforming protein in 1987 (27) and the subsequent elucidation of its participation in the receptor complex for GDNF family ligands (10, 28, 29). Despite having an extracellular domain of more than 600 residues, RET cannot engage any of these ligands directly but requires the auxiliary GFRα receptors for activation (29, 30). Although the RET^{ECD} was known to make direct contacts with both GDNF ligands and GFRα receptors in the complex, binding determinants in the RET^{ECD} molecule and the overall architecture of the complex remained to be characterized.

In this study, we set out to identify functional determinants in the RET^{ECD} responsible for its association with the GDNF-GFRα1 complex using a homologue-scanning mutagenesis approach based on the differential abilities of human and *Xenopus* RET^{ECD} to interact with ligand complexes of mammalian origin. Using this approach, binding determinants were found to be concentrated in the N-terminal CLD1 of the human RET^{ECD}. Within this region, three discrete segments, ranging from 6 to 12 residues (*i.e.* I, III, and V in Fig. 3*A*), could not be replaced by equivalent sequences from *Xenopus* RET^{ECD} without complete loss of activity, indicating that these segments are required for the binding of the human RET^{ECD} to the mammalian GDNF-GFRα1 complex. Importantly, these replacements had no detectable effects on protein production, stability, secretion, or folding, at least at 30 °C. Because of their relatively high solvent accessibility, these epitopes are likely to be directly involved in the interaction of RET with its ligands. When visualized on the modeled three-dimensional structure of the CLD1 (17), regions I, III, and V are all localized on the same face of the model (Fig. 5*A*), delineating a probable surface for interaction with the GDNF-GFRα1 complex. In support of this notion, the only site of *N*-glycosylation known in the human CLD1, namely Asn-98,[2] is located in the opposite side of the

[2] S Kjær, unpublished observations.

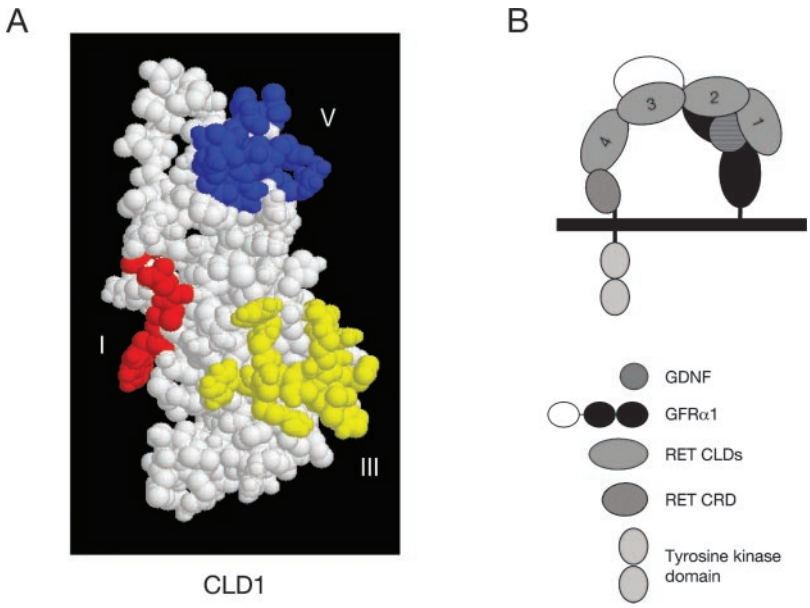

FIG. 5. **Identification of a surface for binding to the GDNF-GFRα1 complex in the RET^{ECD}.** *A*, RasMol (36) representation of the CLD1 of the RET^{ECD} based on the coordinates described by Anders *et al.* (17). Clusters of mutated residues that resulted in complete lack-of-binding of human RET^{ECD} are colored in *red* (region I), *yellow* (region III), and *blue* (region V). Coordinates of the models described in Anders *et al.* (17) are available upon request. *B*, diagram of a tentative model of the ternary complex formed by RET, GFRα1, and GDNF. Although dimers of RET and GFRα1 are believed to interact with the dimeric GDNF ligand, only one of the protomers is shown here for clarity.

domain, a position that is sterically compatible with the proposed location of the ligand binding interface.

Bioinformatics analysis of the RET^{ECD} has recently indicated a structural organization resembling that of classical cadherins with four cadherin-like domains followed by a C-terminal cysteine-rich domain not related to cadherin sequences (17). The x-ray crystal structure of the complete extracellular domain of C-cadherin has recently been solved, revealing an elongated rod-shaped structure (24). Two types of interactions between different cadherin molecules could be defined in these crystals: *cis* interactions were formed laterally between adjacent cadherin molecules, whereas *trans* interactions linked cadherin molecules in opposite orientations, presumably representing the kind of interactions responsible for cell-cell contact. The *trans* interface was defined by a conserved tryptophan side chain (Trp-2) at the N-terminal end of the cadherin molecule from one cell, which was shown to insert into a hydrophobic pocket in the cadherin molecule from the opposing cell (24). The importance of Trp-2 for cadherin-mediated cell adhesion had been inferred independently from structure-function analyses (31). However, Trp-2 is not conserved in RET^{ECD} sequences from different organisms, and no functionally analogous residues can be identified in the modeled structure of the RET^{ECD} (17). Moreover, no adhesive function has to date been attributed to RET molecules (32).

Given the pivotal role played by the CLD1 in the interaction of RET with its ligands, a straight rod-like organization similar to that of classical cadherins would place the major ligand binding site in the RET^{ECD} away from the plasma membrane, where the membrane-anchored GDNF-GFRα1 complex is likely to be. In fact, structure-function studies of the GFRα1 molecule have indicated that the N-terminal domain of this receptor is dispensable for ligand binding and have instead localized the binding determinants toward the middle and C-terminal portions of the molecule (12), in agreement with a membrane-proximal site of complex assembly. How could these apparently contradictory observations be reconciled?

An analogous topological problem has been posed by the cytokine receptor complex formed by gp130, IL-6Rα, and IL-6. Like RET, gp130 has a large multidomain extracellular region, and ligand binding determinants have been localized to the three most N-terminal domains (33). On the other hand, IL-6Rα, like GFRα1, has ligand binding determinants in its membrane-proximal domains (34). A recent crystallographic analysis of the assembly of this complex revealed a bent structure for gp130 and IL-6R with their ligand binding domains forming a "table" that rests on "legs" composed by the more C-terminal domains of the molecules (35). In an analogous fashion, we hypothesize that a bent arrangement of the RET^{ECD} would allow its ligand binding domain to reach the GDNF-GFRα1 complex located closer to the membrane (Fig. 5*B*). It is worth noting that this arrangement would not be possible had the RET^{ECD} retained all the interdomain Ca^{2+} binding sites that characterize classical cadherins. As mentioned previously, the single Ca^{2+} binding site in the RET^{ECD} is located at the interface of CLD2 and CLD3, suggesting a straight and rigid conformation for these two domains. On the other hand, the lack of Ca^{2+} binding sites in all of the other interdomain regions suggest a greater degree of flexibility as compared with classical cadherins that may allow the RET^{ECD} to bend toward the cell membrane. Clearly, validation of this hypothesis awaits the structural determination of the RET^{ECD} in complex with GFRα1 and GDNF.

Acknowledgments—We thank Mart Saarma for the mouse RET cDNA, P. J. Long for the *Xenopus* RET cDNA, Anatoly Sharipo for anti-RET^{ECD} antibodies, and Xiaoli Li for secretarial help.

REFERENCES

1. Lin, L.-F., Doherty, D. H., Lile, J. D., Bektesh, S., and Collins, F. (1993) *Science* **260,** 1130–1132
2. Gash, D. M., Zhang, Z., and Gerhardt, G. (1998) *Ann. Neurol.* **44**, Suppl. 1, S121–S125
3. Eigenbrot, C., and Gerber, N. (1997) *Nat. Struct. Biol.* **4,** 435–438
4. Airaksinen, M. S., and Saarma, M. (2002) *Nat. Rev. Neurosci.* **3,** 383–394
5. Baloh, R. H., Enomoto, H., Johnson, E. M., Jr., and Milbrandt, J. (2000) *Curr. Opin. Neurobiol.* **10,** 103–110
6. Paratcha, G., Ledda, F., and Ibáñez, C. F. (2003) *Cell* **113,** 867–879
7. Edery, P., Eng, C., Munnich, A., and Lyonnet, S. (1997) *BioEssays* **19,** 389–395
8. Santoro, M., Carlomagno, F., Melillo, R. M., Billaud, M., Vecchio, G., and Fusco, A. (1999) *J. Endocrinol. Investig.* **22,** 811–819
9. Carlomagno, F., Devita, G., Berlingieri, M. T., Defranciscis, V., Melillo, R. M., Colantuoni, V., Kraus, M. H., Difiore, P. P., Fusco, A., and Santoro, M. (1996) *EMBO J.* **15,** 2717–2725
10. Trupp, M., Arenas, E., Fainzilber, M., Nilsson, A.-S., Sieber, B. A., Grigoriou, M., Kilkenny, C., Salazar-Grueso, E., Pachnis, V., Arumäe, U., Sariola, H., Saarma, M., and Ibáñez, C. F. (1996) *Nature* **381,** 785–789
11. Trupp, M., Raynoschek, C., Belluardo, N., and Ibáñez, C. F. (1998) *Mol. Cell Neurosci.* **11,** 47–63
12. Scott, R. P., and Ibáñez, C. F. (2001) *J. Biol. Chem.* **276,** 1450–1458
13. Eketjäll, S., Fainzilber, M., Murray-Rust, J., and Ibáñez, C. F. (1999) *EMBO J.* **18,** 5901–5910
14. Baloh, R. H., Tansey, M. G., Johnson, E. M., and Milbrandt, J. (2000) *J. Biol. Chem.* **275,** 3412–3420
15. Shi, Y. G., and Massague, J. (2003) *Cell* **113,** 685–700
16. Sanicola, M., Hession, C., Worley, D., Carmillo, P., Ehrenfels, C., Walus, L., Robinson, S., Jaworski, G., Wei, H., Tizard, R., Whitty, A., Pepinsky, R. B.,

and Cate, R. L. (1997) *Proc. Natl. Acad. Sci. U. S. A.* **94,** 6238–6243
17. Anders, J., Kjær, S., and Ibáñez, C. F. (2001) *J. Biol. Chem.* **276,** 35808–35817
18. Kjær, S., and Ibáñez, C. F. (2003) *Hum. Mol. Genet.* **12,** 2133–2144
19. Horton, R. M., Hunt, H. D., Ho, S. N., Pullen, J. K., and Pease, L. R. (1989) *Gene* (*Amst.*) **77,** 61–68
20. Fraczkiewicz, R., and Braun, W. (1998) *J. Comput. Chem.* **19,** 319–333
21. van Weering, D., Moen, T. C., Braakman, I., Baas, P. D., and Bos, J. L. (1998) *J. Biol. Chem.* **273,** 12077–12081
22. Nozaki, C., Asai, N., Murakami, H., Iwashita, T., Iwata, Y., Horibe, K., Klein, R. D., Rosenthal, A., and Takahashi, M. (1998) *Oncogene* **16,** 293–299
23. Nagar, B., Overduin, M., Ikura, M., and Rini, J. M. (1996) *Nature* **380,** 360–364
24. Boggon, T. J., Murray, J., Chappuis-Flament, S., Wong, E., Gumbiner, B. M., and Shapiro, L. (2002) *Science* **296,** 1308–1313
25. Bogan, A. A., and Thorn, K. S. (1998) *J. Mol. Biol.* **280,** 1–9
26. Steen, M., Villoutreix, B. O., Norstrom, E. A., Yamazaki, T., and Dahlback, B. (2002) *J. Biol. Chem.* **277,** 50022–50029
27. Takahashi, M., and Cooper, G. M. (1987) *Mol. Cell Biol.* **7,** 1378–1385
28. Durbec, P., Marcos-Gutierrez, C. V., Kilkenny, C., Grigoriou, M., Suvanto, P., Wartiovaara, K., Smith, D., Ponder, B., Costantini, F., Saarma, M., Sariola, H., and Pachnis, V. (1996) *Nature* **381,** 789–792
29. Jing, S. Q., Wen, D. Z., Yu, Y. B., Holst, P. L., Luo, Y., Fang, M., Tamir, R., Antonio, L., Hu, Z., Cupples, R., Louis, J. C., Hu, S., Altrock, B. W., and Fox, G. M. (1996) *Cell* **85,** 1113–1124
30. Treanor, J., Goodman, L., Desauvage, F., Stone, D. M., Poulsen, K. T., Beck, C. D., Gray, C., Armanini, M. P., Pollock, R. A., Hefti, F., Phillips, H. S., Goddard, A., Moore, M. W., Buj-Bello, A., Davies, A. M., Asai, N., Takahashi, M., Vandlen, R., Henderson, C. E., and Rosenthal, A. (1996) *Nature* **382,** 80–83
31. Tamura, K., Shan, W. S., Hendrickson, W. A., Colman, D. R., and Shapiro, L. (1998) *Neuron* **20,** 1153–1163
32. Takahashi, M., Asai, N., Iwashita, T., Isomura, T., Miyazaki, K., and Matsuyama, M. (1993) *Oncogene* **8,** 2925–2929
33. Hammacher, A., Richardson, R. T., Layton, J. E., Smith, D. K., Angus, L. J., Hilton, D. J., Nicola, N. A., Wijdenes, J., and Simpson, R. J. (1998) *J. Biol. Chem.* **273,** 22701–22707
34. Yawata, H., Yasukawa, K., Natsuka, S., Murakami, M., Yamasaki, K., Hibi, M., Taga, T., and Kishimoto, T. (1993) *EMBO J.* **12,** 1705–1712
35. Boulanger, M. J., Chow, D. C., Brevnova, E. E., and Garcia, K. C. (2003) *Science* **300,** 2101–2104
36. Sayle, R., and Milner-White, E. (1995) *Trends Biochem. Sci.* **20,** 374–376

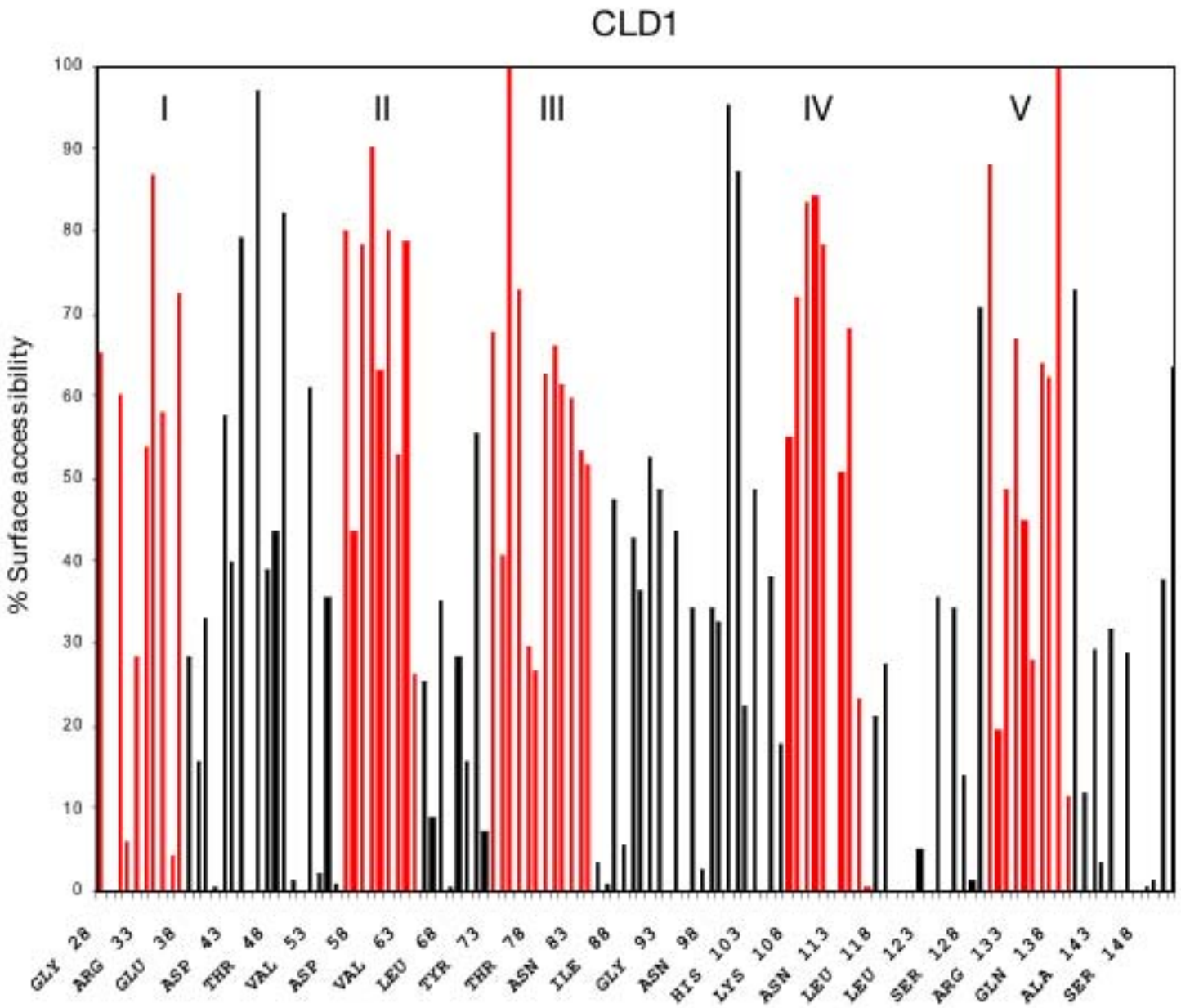
CLD1
% Surface accessibility
100
90
80
70
60
50
40
30
20
10
0
I
II
III
IV
V
GLY 28
ARG 33
GLU 38
ASP 43
THR 48
VAL 53
ASP 58
VAL 63
LEU 68
TYR 73
THR 78
ASN 83
ILE 88
GLY 93
ASN 98
HIS 103
LYS 108
ASN 113
LEU 118
LEU 123
SER 128
ARG 133
GLN 138
ALA 143
SER 148

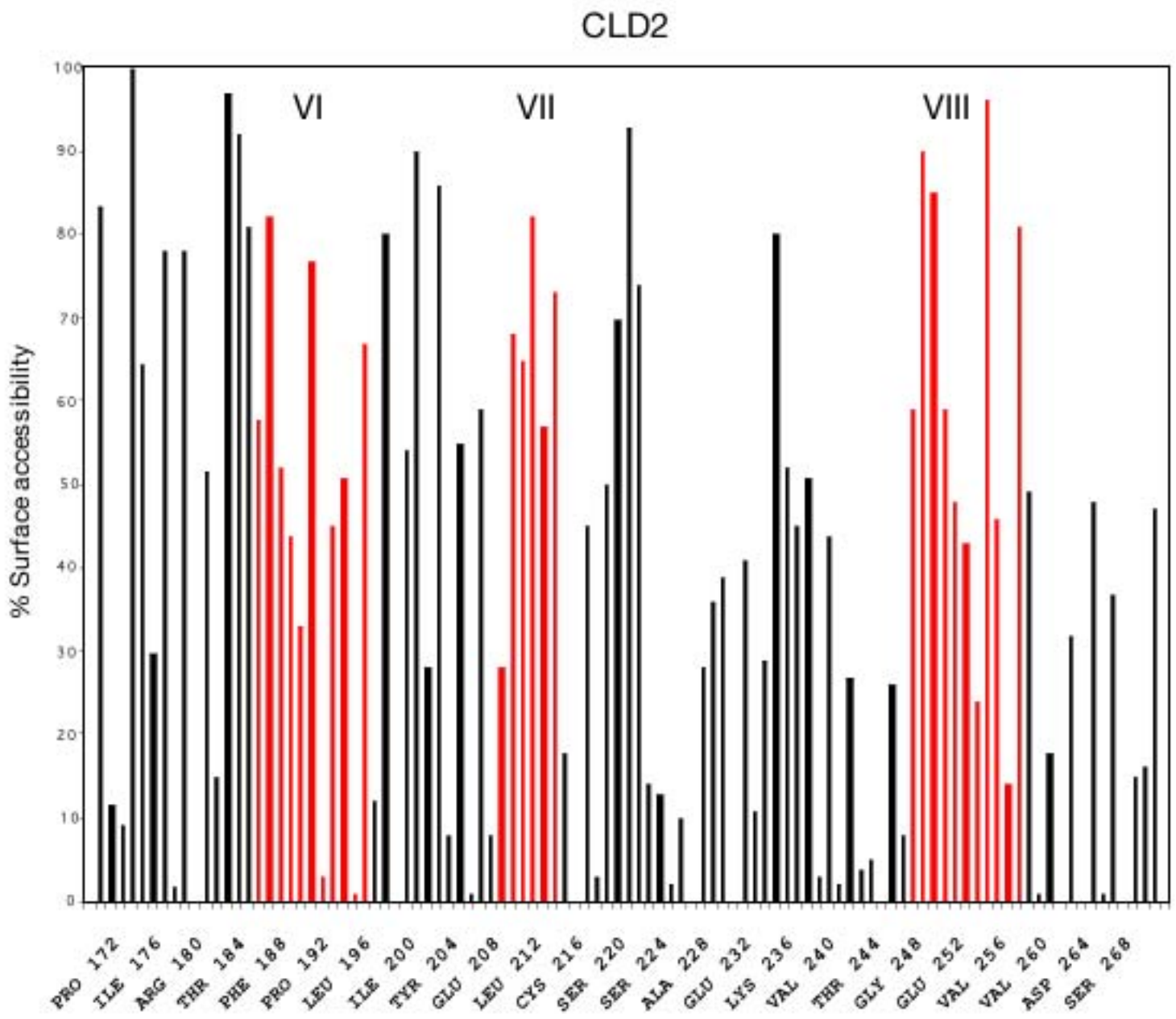
CLD2
VI
VII
VIII
% Surface accessibility
0
10
20
30
40
50
60
70
80
90
100
PRO 172
ILE 176
ARG 180
THR 184
PHE 188
PRO 192
LEU 196
ILE 200
TYR 204
GLU 208
LEU 212
CYS 216
SER 220
SER 224
ALA 228
GLU 232
LYS 236
VAL 240
THR 244
GLY 248
GLU 252
VAL 256
VAL 260
ASP 264
SER 268

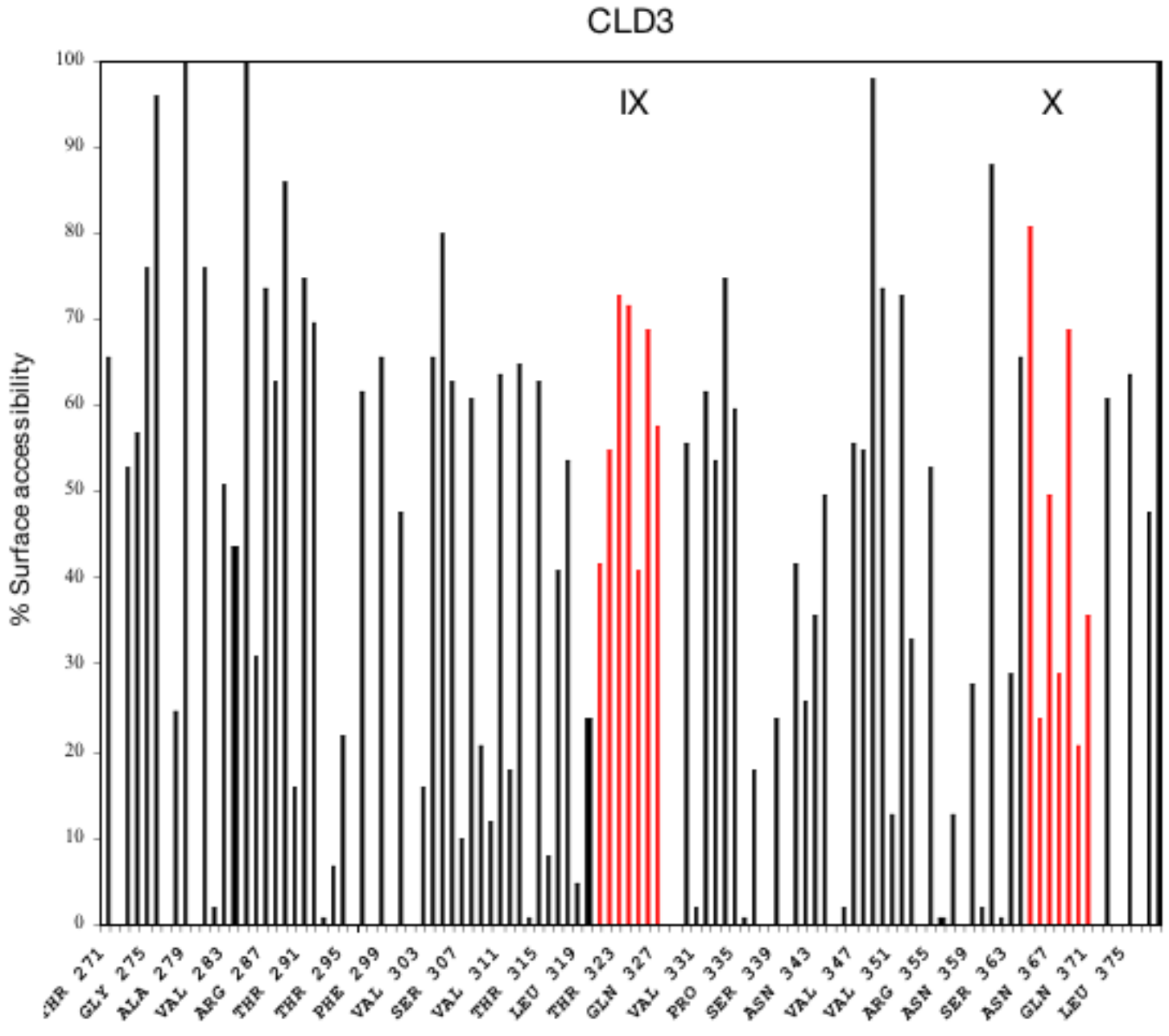
CLD3
IX
X
% Surface accessibility
100
90
80
70
60
50
40
30
20
10
0
THR 271
GLY 275
ALA 279
VAL 283
ARG 287
THR 291
THR 295
PHE 299
VAL 303
SER 307
VAL 311
THR 315
LEU 319
THR 323
GLN 327
VAL 331
PRO 335
SER 339
ASN 343
VAL 347
VAL 351
ARG 355
ASN 359
SER 363
ASN 367
GLN 371
LEU 375